

## Experimental Study of the Principles Governing Tokamak Transport

F. Wagner, O. Gruber, K. Lackner, H. D. Murmann, E. Speth, G. Becker, H. S. Bosch, H. Brocken, G. Cattanei, D. Dorst, A. Eberhagen, A. Elsner, V. Erckmann, G. Fussmann, O. Gehre, J. Gernhardt, G. v. Gierke, E. Glock, G. Grieger, P. Grigull, G. Haas, H. Hacker, H. J. Hartfuss, H. Jäckel, R. Jaenicke, G. Janeschitz, J. Junker, F. Karger, W. Kasperek,<sup>(a)</sup> M. Keilhacker, M. Kick, O. Klüber, M. Kornherr, H. Kroiss, M. Kuehner, M. Lenoci, G. Lisitano, M. Maassberg, C. Mahn, S. Marlier, H. M. Mayer, K. McCormick, D. Meisel, V. Mertens, E. R. Müller, G. Müller, G. Müller,<sup>(a)</sup> H. Niedermeyer, W. Ohlendorf, W. Poschenrieder, H. Rapp, F. Rau, H. Renner, H. Riedler, H. Ringler, F. Sardei, P. G. Schüller,<sup>(a)</sup> K. Schwörer,<sup>(a)</sup> G. Siller, F. Söldner, K.-H. Steuer, M. Thumm,<sup>(a)</sup> M. Tutter, O. Vollmer, A. Weller, R. Wilhelm,<sup>(a)</sup> H. Wobig, E. Würsching, and M. Zippe

Max-Planck-Institut für Plasmaphysik, EURATOM Association, D-8046 Garching, Federal Republic of Germany  
(Received 4 February 1986)

Both in Ohmically and beam-heated  $L$ -mode discharges of ASDEX, the electron-temperature ( $T_e$ ) profile shape can be varied over a wide range by the choice of the safety factor  $q_a$ . The power-deposition profile, on the contrary, has no effect on the  $T_e$  profile shape. In current-free W-VII-A stellarator plasmas, no such invariance property is found. An independent constraint seems to fix the current distribution  $j(r)$  of the tokamak, which defines the conditions of electron heat transport.

PACS numbers: 52.25.Fi, 52.55.Fa

The electron-heat-transport mechanisms in a tokamak are still not understood after two decades of concentrated efforts. Mostly Ohmically heated (OH) plasmas have been studied in the past.<sup>1</sup> Auxiliary heating, successfully applied in the last few years, caused distinct changes in the confinement properties and offered the possibility of reconsidering the dominant features of tokamak transport: Auxiliary heating changes the scaling of the global energy-confinement time  $\tau_E$  from density to plasma current as the leading scaling parameter.<sup>2</sup> Furthermore, a degradation in  $\tau_E$  with auxiliary heating power is generally observed<sup>2</sup> irrespective of the heating method ( $L$  mode), while divertor tokamaks can operate with neutral-injection (NI) heating in a regime of good confinement ( $H$  mode).<sup>3</sup> This paper presents an analysis of plasma profiles of the asymmetric-divertor tokamak ASDEX with NI heating and confronts the tokamak observations with those from the Wendelstein (W) VII-A stellarator with electron-cyclotron-resonance heating (ECRH).<sup>4</sup>

In Ohmically heated plasmas the plasma profile shapes for density ( $n_e$ ) and temperatures ( $T_e, T_i$ ) can easily be varied by a change of the ratio of toroidal field  $B_T$  to plasma current  $I_p$  (corresponding to a change in the safety factor  $q_a$ ). At a large  $q_a$  value, the profiles are peaked and the gradients in the insulation zone (between  $q = 1$  and the periphery affected by atomic processes) are mostly flat; at low  $q_a$  (with extended  $q = 1$  zone), the profiles are broad and the gradients are steep. Figure 1(a) shows the ratio of peak to volume-averaged electron temperature versus  $q_a$

(open and solid circles are the Ohmic values) for two different line-averaged density values. The  $T_e$  profile shape shows a strong dependence on  $q_a$ . In clean Ohmic discharges as provided by the divertor configuration and under steady-state conditions, the  $T_e$  profile is linked resistively to the current distribution and reflects its  $q_a$  dependence. The current distribution, however, largely determines the Ohmic-heating-power profile. As the  $T_e$  profile follows the power-deposition

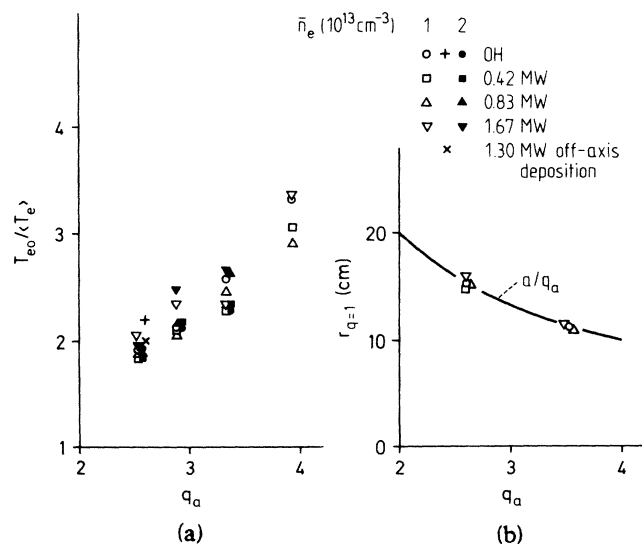


FIG. 1. (a) Ratio of central to volume-averaged electron temperature and (b) radius of the  $q = 1$  surface vs cylinder  $q_a$  at different densities and beam heating power.

profile in Ohmic discharges, it seemed justified to base the transport analysis of tokamak discharges on diffusive transport and to aim at determination of local transport coefficients and their dependence on local parameters

Figure 1(a) also shows the ratio of peak to volume-averaged electron temperature for various beam powers in the  $L$  regime. The  $T_e$  profile shapes hardly change with beam power but can still be varied by the choice of  $q_a$  to the same extent as in Ohmic discharges. It is important to note that with auxiliary heating the relative  $T_e$  gradients  $d \ln T_e / dr$  and not the absolute gradients remain invariant. The invariance of the  $T_e$  profile during NI has also been observed by others<sup>5</sup> and has been dubbed "profile consistency."<sup>6</sup> This invariance property has further been confirmed in density scans of Ohmically and beam-heated ASDEX discharges where  $T_{e0}$  was changed by a factor  $>3$ , while  $T_{e0} / \langle T_e \rangle$  values scattered between 2.1 and 2.6 ( $q_a = 2.8$ ). The invariance of the logarithmic derivative (and not the absolute gradient) has been further confirmed in OH discharges by comparison of a clean discharge ( $T_{e0} = 1.0$  keV) with one polluted by neon ( $T_{e0} = 2.2$  keV).

The invariance of the  $T_e$  profile even at high beam power with negligible Ohmic power input indicates that the  $T_e$  profile is not determined by the power-deposition profile—as first concluded from the consideration of Ohmic discharges alone. The lack of dependence of the  $T_e$  profile shape on the heat-deposition profile has been tested in two extreme cases. A peaked deposition profile was realized by high-velocity beam injection ( $H^0$ , 42 keV) into a low-

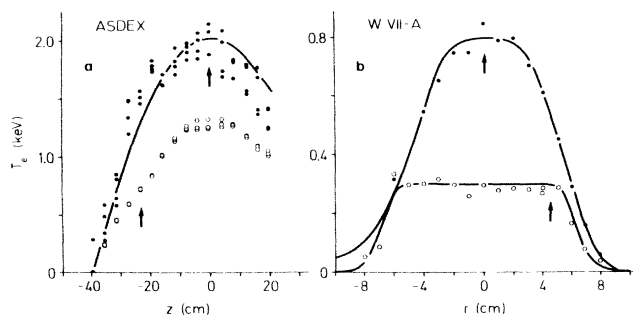


FIG. 2. Electron-temperature profiles (a) of ASDEX tokamak plasmas with peaked beam-power deposition (dots;  $\bar{n}_e = 0.9 \times 10^{13} \text{ cm}^{-3}$ ,  $H^0 \rightarrow D^+$  at 42 keV) and off-axis deposition (circles;  $\bar{n}_e = 5 \times 10^{13} \text{ cm}^{-3}$ ,  $D^0 \rightarrow H^+$  at 29 keV) and (b) of currentless W-VII-A stellarator plasmas with ECRH at  $2\omega_{ce}$ : ECRH  $\sim 0.1$  MW;  $f = 70$  GHz;  $\bar{n}_e = 2.2 \times 10^{13} \text{ cm}^{-3}$ ;  $B_T = 1.26\text{--}1.28$  T. The arrows indicate the maxima of the auxiliary-heating-power deposition; the solid curve is a fit by the lower curve matched to the central value of the upper profile to demonstrate the profile invariance of the two cases.

density discharge ( $\bar{n}_e = 0.9 \times 10^{13} \text{ cm}^{-3}$ ); the width of the centrally peaked deposition profile was  $\sim 14$  cm. The other extreme—low-velocity injection ( $D^0$ , 29 keV) into a high-density plasma ( $\bar{n}_e = 5 \times 10^{13} \text{ cm}^{-3}$ )—yielded a hollow beam-deposition profile peaked at  $r = 0.65a$  [the deposition profile is shown in Fig. 3(a)]. The  $T_e$  profiles are plotted in Fig. 2(a) (the deposition maxima being indicated by arrows). The solid line is the fit through the lower profile, but normalized to the peak value of the higher one: The profile shape is hardly affected by the large differences between the heat-deposition profiles.

ECRH experiments in W-VII-A<sup>4</sup> reveal that a different mechanism determines plasma profile shapes and consequently transport in a current-free stellarator. Figure 2(b) shows the variation of the  $T_e$  profiles at different locations of the ECRH power-deposition region. The deposition width is typically 5 cm. The  $T_e$  profiles are indeed flat inside the zone of no power deposition and show steep gradients outside the radius of power deposition. Detailed transport analysis<sup>4</sup> confirms that the stellarator profiles are governed by the expected transport principles where the heat conduction coefficient is given (dependent on local parameters such as  $B_0$ ,  $\iota$ ,  $n_e$ , and  $T_e$ ) and the gradients adjust according to the heat flux.

The different constraints on the  $T_e$  profiles of the ASDEX tokamak and currentless W-VII-A stellarator discharges point to the current distribution as the dominant element which shapes the tokamak profiles. The invariance of the current profile is confirmed by the analysis of the sawtooth inversion radius in ASDEX. The radius of the  $q = 1$  surface is found to vary with  $q_a$  according to  $a/q_a$  but otherwise is not dependent on heating power [see Fig. 1(b)], indicating that an invariant fraction of the plasma current flows within the  $q = 1$  surface.

Normally, auxiliary heating leads to enhanced power input and  $\chi_e$  increases. On the other hand, even in the  $L$  regime an injection scenario is possible where at least core confinement does not degrade.<sup>7</sup> With low-velocity NI (29 keV,  $D^0$ ) into a high-density hydrogen discharge ( $\bar{n}_e = 5 \times 10^{13} \text{ cm}^{-3}$ ), the beam-power-deposition profile is hollow with small central heating. The calculated power-deposition profile  $P$  is shown in Fig. 3(a) together with that of a control series (same  $I_p$  and  $B_T$ ) of high beam velocity (42 keV,  $H^0$ ) into a deuterium discharge of the same density. The different central power densities in the two cases are confirmed by the different rates with which  $T_e$  increases after a sawtooth fall: With hollow deposition,  $dT_e/dt$  is the same as in the Ohmic phase; in the peaked-deposition case, it doubles. In both cases a similar H-D species mix of the plasma was aimed for in order to compensate for the isotope effect on global confinement<sup>8</sup> as far as possible. Figure 3(a) also shows the energy-

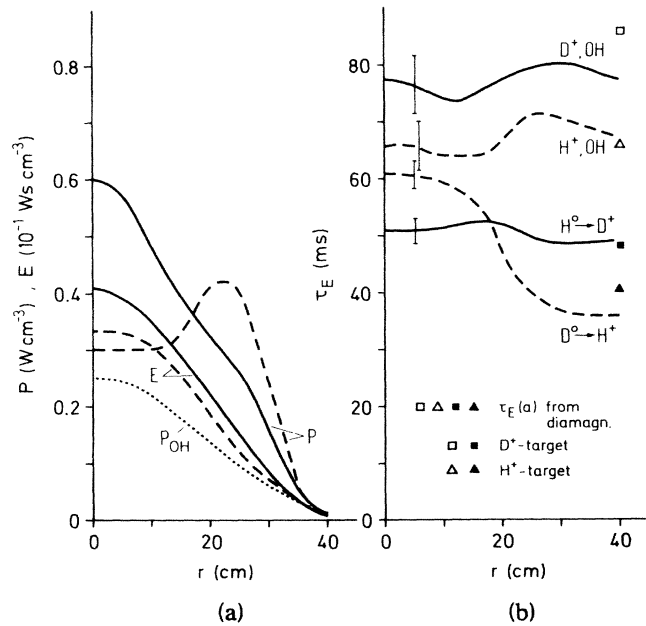


FIG. 3. (a) Energy-density and beam-power-deposition profiles for central (solid lines;  $H^0 \rightarrow D^+$ , 42 keV) and off-axis (dashed line;  $D^0 \rightarrow H^+$ , 29 keV) deposition;  $\bar{n}_e = 5 \times 10^{13} \text{ cm}^{-3}$ . The dotted curve is the Ohmic power during NI. (b) Radial dependence of the global energy-confinement time for the two cases; the symbols represent the values from the diamagnetic loop.

density profile  $E$  from individually measured  $T_e$ ,  $n_e$ , and  $T_i$  profiles. Even with off-axis deposition cases, the  $T_e$  profile is peaked and obeys the profile-invariance constraint [see Fig. 1(a)]. Figure 3(b) shows the radial variation of the energy-confinement time

$$\tau_E(r) = \int_0^r E r' dr' / \int_0^r P r' dr'$$

for the two beam cases together with the Ohmic dependence. The global  $\tau_E$  values obtained from plasma diamagnetism are also shown. In the peaked-deposition case, the confinement is degraded over the whole cross section; in the off-axis case, the local  $\tau_E$  is high in the plasma center.

The dominant profile effect of a tokamak discharge seems to be the invariance of the current distribution, which is not affected by the heating method or the details of the power-deposition profile. As the local  $T_e$  gradients are specified at the steady-state conditions by the superimposed constraint, the heat flow in the insulation zone occurs with NI, as in Ohmic plasmas, basically via low gradients at high  $q_a$  and via steep ones at low  $q_a$ . As the gradients cannot adjust according to the local heat flux, the thermal diffusivity must change in order to yield steady-state conditions. Therefore, the case with low central power deposition needs low central transport; the one with high central deposition re-

quires high transport and yields low confinement. The global  $\tau_E$  values, however, are similarly reduced in comparison to the OH phase. (The difference in the global values might be due to a residual different species mix.)

The possibility of the plasma rapidly adjusting  $\chi_e$  to match the heat flux requirements is observed in rapid sawtooth propagation,<sup>9</sup> which frequently occurs much faster than expected from the  $\chi_e$  of the undisturbed plasma; another example is the rapid degradation of confinement in the case of beam heating, which sets in typically after one ion slowing-down time. After a sawtooth drop, the plasma is forced to transport a high power flux; with beam heating, the degradation occurs as soon as power is deposited even though it may still be in the neighborhood of OH plasma parameters. It is important to note that  $\chi_e$  obtained from the propagation of ECRH-produced heat pulses matched the  $\chi_e$  of the undisturbed equilibrium plasma in the case of current-free W-VII-A discharges.<sup>10</sup>

Because of the global constraint, the definition of a local heat transport coefficient with a dependence on local plasma parameters does not seem to be appropriate;  $\chi_e$  directly depends on the heating power. Consequently, the improved central confinement in the hollow-deposition case is only maintained as long as the local power flux is low, and it does not seem to be an easy solution to the problems caused by the deterioration of global energy confinement.

Profile consistency as described above concerns only the logarithmic temperature derivative and therefore allows no statement about absolute temperature levels and total confinement times. For these to be determined, a relationship between absolute local plasma parameters and the locally passing heat flux has to exist in some region in space. The lack of any dependence of the energy content on power-deposition profiles, as observed in our NI experiments, suggests placement of this region outside the deposition zone, where the passing energy flux remains constant for these cases. This would give dominant importance to the confinement properties in the boundary region.<sup>11</sup> This is consistent with the observed strong improvement in overall confinement accompanying the formation of an edge temperature pedestal in  $H$ -regime discharges.<sup>12</sup>

The outstanding feature of all tokamak experiments with strong additional heating is the apparent change in magnitude and scaling of confinement times compared with purely Ohmic discharges. Scaling might be determined by processes in the postulated boundary loss region, or, in its major trends, by the profile constraint. At high heating power—when the plasma current does not contribute to heating— $\tau_E \propto I_p$  is found irrespective of the auxiliary heating method. The variation of the otherwise invariant  $T_e$  profile

shape with  $q_a$ —shrinking towards higher  $q_a$  at constant central value—might lead to current scaling. Under Ohmic conditions, however, when the heating power increases with current, profile invariance might cause a largely current-independent scaling. In this view,  $\tau_E \propto I_p$  is not the result of a new transport property which is common to all auxiliary heating methods; it seems more plausible that it is the result of a common feature of auxiliary heating, namely the loss of dominance of the Ohmic power input. Consequently, at low beam power, a mix of Ohmic- and auxiliary-heating scaling elements is observed in  $\tau_E$  scaling.<sup>8</sup>

The actual microscopic mechanism which provides invariant current-density profiles at the expense of the thermal transport (increasing with the thermal flux to be transported) is not yet known. However, experimental observations yield some important clues: Energy- and particle-confinement degradation are always correlated (in the case of ASDEX also with counter NI); the sudden degradation in confinement shortly after firing of the beams causes a rapid loss of runaway electrons, pointing to strong magnetic turbulence; the comparison of hydrogen, deuterium, and helium discharges reveals as a common feature of high-density Ohmic- and auxiliary-heated plasmas (geometrical parameters excluded) an increase of the *electron* thermal diffusivity (at constant  $B_T$ ) with either decreasing *ion* Larmor radius or increasing sound velocity.

The interest and encouragement shown by the Fachbeirat of the Max-Planck-Institut für Plasmaphysik and

in particular by H. Furth are gratefully acknowledged.

<sup>(a)</sup>Permanent address: Institut für Plasmaforschung der Universität Stuttgart, Stuttgart, West Germany.

<sup>1</sup>J. Hugill, Nucl. Fusion **23**, 331 (1983).

<sup>2</sup>S. M. Kaye and R. J. Goldston, Nucl. Fusion **25**, 65 (1985).

<sup>3</sup>F. Wagner *et al.*, Phys. Rev. Lett. **49**, 1408 (1982).

<sup>4</sup>G. Grieger *et al.*, Plasma Phys. Controlled Fusion **28**, 43 (1986).

<sup>5</sup>R. J. Goldston, Plasma Phys. Controlled Fusion **26**, 87 (1984).

<sup>6</sup>B. Coppi, Comments Plasma Phys. Controlled Fusion **5**, 261 (1980).

<sup>7</sup>E. Speth *et al.*, in Proceedings of the Twelfth European Conference on Controlled Fusion and Plasma Physics, Budapest, 1985 (unpublished), Vol. II, p. 284. Similar observations were made in pellet-refueled discharges of the Princeton tokamak fusion test reactor by M. Murakami *et al.*, Plasma Phys. Controlled Fusion **28**, 17 (1986).

<sup>8</sup>F. Wagner *et al.*, in Proceedings of the Twelfth European Conference on Controlled Fusion and Plasma Physics, Budapest, 1985 (unpublished), Vol. II, p. 284.

<sup>9</sup>The fast sawtooth propagation is observed in several tokamaks; see, e.g., Equipe TFR, in *Proceedings of the Ninth International Conference on Plasma Physics and Controlled Nuclear Fusion Research, Baltimore, 1982* (International Atomic Energy Agency, Vienna, 1983), Vol. 3, p. 383; E. D. Fredrickson *et al.*, to be published.

<sup>10</sup>H. J. Hartfuss *et al.*, Nucl. Fusion (to be published).

<sup>11</sup>H. Furth, in Proceedings of the Summer School on Basic Physical Processes of Toroidal Fusion Plasmas, Varenna, 1985 (unpublished).

<sup>12</sup>F. Wagner *et al.*, Phys. Rev. Lett. **53**, 1453 (1984).